Investigation of scattering processes in a laser plasma

V. L. Artsimovich, L. M. Gorbunov, Yu. S. Kas'yanov, and V. V. Korobkin

P. N. Lebedev Physics Institute, Academy of Sciences of the USSR, Moscow
(Submitted 20 November 1980)
Zh. Eksp. Teor. Fiz. **80**, 1859–1867 (May 1981)

Laser radiation scattered at various angles was subjected to a spectral time-resolved study at the fundamental frequency ω_0 and at the frequency of the second harmonic $2\omega_0$. The study was carried out for normal and oblique incidence of the radiation from a single-frequency neodymium laser on plane targets. The processes governing the scattered-light spectrum and the dynamics of a plasma corona were analyzed.

PACS numbers: 52.25.Ps

I. INTRODUCTION

Light scattering in a plasma corona is an important factor which reduces the efficiency of target heating. This is the main reason for investigating the scattering of highpower laser radiation by a plasma.

Studies of the spectral composition of the scattered radiation and particularly the use of time resolution in such studies are necessary conditions for revealing the role of any particular scattering mechanism.[1-6]

We shall report the results of spectral time-resolved measurements on laser radiation scattered at various angles at the fundamental frequency ω_0 and at the second-harmonic frequency $2\omega_0$. The measurements were made for normal and oblique incidence of neodymium laser radiation on plane polyethylene and aluminum targets. The experimental results were used in a study of the processes governing the scattered radiation spectrum and possible dynamics of the plasma corona.

II. EXPERIMENTAL METHOD

Use was made of a neodymium-glass laser system shown schematically in Fig. 1. A single-frequency glass laser with passive Q switching[7] was used as a master oscillator 1. Laser pulses were shaped in a system comprising a double Pockels cell 2, which made it possible to achieve a high contrast (up to 10^5) of the output radiation and to vary continuously the duration of laser pulses from 2 to 8 nsec. A spatial filter 3 consisting of two spherical mirrors (radii of curvature 5 m) and an aperture ($D \approx 1.5$ mm) made it possible to improve the spatial resolution and to reduce the laser beam divergence. One four-pass (A_1) and three one-pass (A_2, A_3, and A_4) amplifiers of the UMI-35 type (with active elements 30 mm in diameter) represented the preliminary amplifying stage. A Faraday isolator 4 protected the optical components of the apparatus from damage by the radiation reflected from the laser plasma. Two one-pass amplifiers (A_5 and A_6) of the GOS-1001 type (rod diameters 45 mm) formed the final amplifying stage.

The main instrumental parameters used in the measurements were as follows: the radiation energy was up to 30 J, the pulse duration was 5 nsec, and the contrast was $\sim 3\times10^4$.

Laser radiation was focused by an $f/6$ lens ($f=300$ mm) on the surface of a solid plane target in a vacuum chamber (Fig. 2). Targets were massive disks 30 mm in diameter and up to 5 mm thick all tightly pressed on the same axle. The laser radiation was focused on a side surface of a disk. This made it possible to replace a target without disturbing the vacuum in the chamber and also to vary easily the angle of incidence of laser radiation on the target. Rotation of the axle altered the position of the target surface relative to the focus by no more than 50 μ.

The distribution of the radiation intensity on the target surface was measured by two methods using lenses identical with the focusing lens in the vacuum chamber. In one method (4 in Fig. 2) a focusing "spot" was projected with $\sim 20\times$ magnification on the photocathode of an image-converter camera, whereas in the second method (3 in Fig. 2) use was made of a mirror wedge similar to that described, for example, in Ref. 8. In

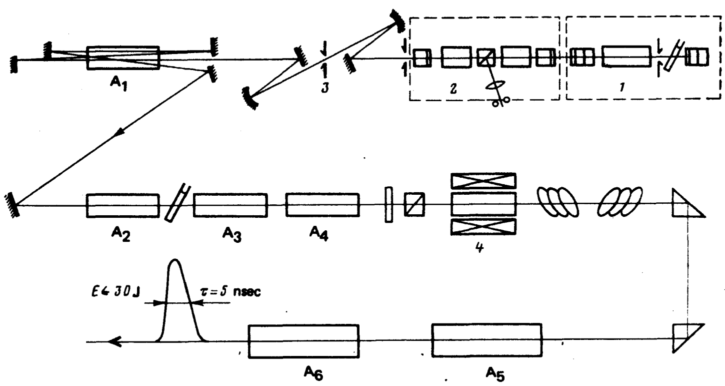

FIG. 1. Optical part of the laser system.

 0038-5646/81/050963-05$02.40

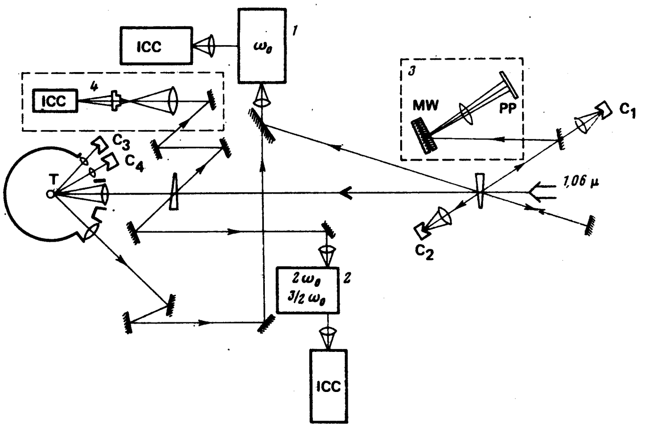

FIG. 2. Experimental setup for normal incidence of laser radiation on a target: T is a target, C_{1-4} are calorimeters; 1) SFD-1 monochromator; 2) MDR-3 monochromator; 3), 4) systems for the determination of the distribution of the laser radiation intensity on a target; PP is a photographic plate; MW is a mirror wedge; ICC is an image-converter camera.

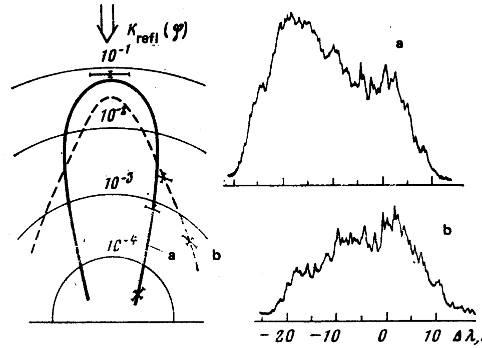

FIG. 3. Angular distributions and microphotograms of backscattered radiation.

the first method the range of the measured intensities was governed by the dynamic range of the system formed by the camera and the photographic film, which usually did not exceed ~30, whereas in the second method this range was ~10^3–10^4; the maximum power density q which could be measured by these methods was $(4-6)\times 10^{14}$ W/cm². The power density q was varied by altering the laser pumping or by moving a target along the optic axis of the focusing system (defocusing).

Time-resolved spectra, and the energy and angular characteristics of the plasma-scattered laser radiation were investigated using the following apparatus (Fig. 2).

1. In the fundamental frequency region use was made of an SFD-1 monochromator coupled to an image-converter camera of the UMI-92 type with an S-1 photocathode. Dispersion on the photographic film was ~10 Å/mm, the spectral resolution was 0.5 Å, and the time resolution was ~10^{-10} sec.

2. In the region of the harmonics $2\omega_0$ and $3\omega_0/2$ use was made of an MDR-3 monochromator coupled to an image-converter camera of the UMI-93 type with an S-20 or S-1 photocathode. The dispersion was 12.5 Å/mm or 25 Å/mm, depending on the selected diffraction grating. The spectral resolution was 0.6 or 1.2 Å, and the time resolution was 10^{-10} sec. Both image-converter cameras were operated synchronously in the streak (scanning) mode.

3. The size of the focusing spot was monitored with a PIM-3 image-converter camera.

4. The incident and scattered energies were measured using KIM and IKT calorimeters.

III. NORMAL INCIDENCE OF LASER RADIATION ON A TARGET

Investigations of backscattered radiation at the fundamental frequency had been made earlier (see Refs. 5 and 9) at power densities of $q = 10^{12}-6\times 10^{14}$ W/cm². They showed that in the range $q < 3\times 10^{13}$ W/cm² the spectrum had only the red wing whose width increased on increase on q. In the range $q > 3\times 10^{13}$ W/cm² the blue part of the spectrum appeared after a time delay. The intensity of the blue component decreased rapidly on increase in q. Moreover, the scattering spectrum recorded for $q > 10^{14}$ W/cm² had certain special features.[9] In particular, at the beginning of a pulse a short-lived wide wing appeared in the red part of the spectrum. In the present section we shall give the results of a more detailed investigation of the scattered radiation in the case when $q > 10^{14}$ W/cm².

The spectrum of the scattered light and the scattering coefficients were determined at the fundamental frequency for normally incident laser radiation and this was done at three angles of observation: 0° (backscattering), 22°, and 45°. Measurements of the scattering coefficients indicated that in the range $q > 10^{14}$ W/cm² the angular distribution was fairly narrow. The width of this distribution decreased on increase in the intensity of the blue component in the scattered-radiation spectrum. Figure 3 shows microphotograms of the spectra obtained for different shots and the corresponding angular distributions. All these results were obtained for polyethylene targets in the power density range $q \sim (4-5)\times 10^{14}$ W/cm².

Figure 4 shows spectrograms of backscattered radia-

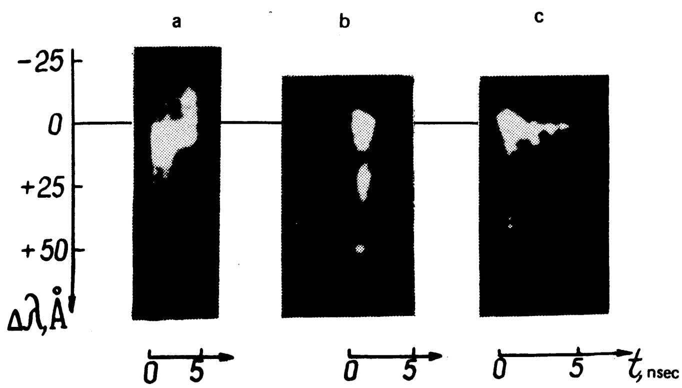

FIG. 4. Time-resolved spectrograms of radiation scattered at the fundamental frequency for normal incidence and three observation angles: a) backscattering; b) 45°; c) 22°.

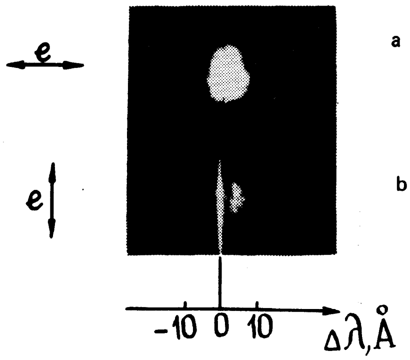

FIG. 5. Spectrograms of backscattered radiation at the fundamental frequency for two polarizations (relative to the polarization of the incident laser radiation): a) perpendicular; b) parallel.

tion (a) and of the radiation scattered at angles of 22° (c) and 45° (b), obtained for the same shot with $q > 4 \times 10^{14}$ W/cm^2 reaching a polyethylene target. All these spectrograms exhibited an initial short-lived but considerable broadening (up to 70 Å) in the red direction with a distinguishable fine structure ($\Delta\lambda \sim 1-3$ Å). Scattering at the angle of 22° continued practically throughout the laser pulse (Fig. 4c), but it was much shorter at the angle 45° (Fig. 4b). The blue part of the spectrum was observed only in the backscattered radiation and the intensity maximum occurred in the second half of the pulse (Fig. 4a). A similar time dependence of the blue component in the backscattered radiation was observed also earlier[2] under experimental conditions very similar to ours. The relatively weak ($\Delta\lambda \sim 5$ Å) blue broadening at the beginning of the scattered pulse was clearly associated with the motion of a critical-density plasma away from the target.

An investigation of the polarization of the backscattered radiation (Fig. 5) showed that whereas the blue component had the same polarization identical as the incident radiation (Fig. 5b), the red component was largely depolarized (Figs. 5a and 5b).

IV. OBLIQUE INCIDENCE OF LASER RADIATION ON A TARGET

Processes responsible for the formation of the scattered-radiation spectrum were studied by carrying out measurements at the frequencies ω_0 and $2\omega_0$ also at oblique incidence. Spectrograms were obtained for the angle of incidence 22° and for three observation angles: backscattering, specular, and normal to the target (Fig. 6). Broadening of the spectrum in the red direction at the beginning of a pulse occured for all the observation angles not only near the frequency ω_0 but also at $2\omega_0$. The scattering along the normal to the target was observed briefly for a time approximately equal to the lifetime of the broadened red part of the spectrum. In the specular direction the red broadening at the beginning of a pulse was followed by a relatively narrow line near ω_0. A strong blue component appeared with time in the backscattered radiation.

Measurements carried out using the s and p polarizations of the incident light produced no significant

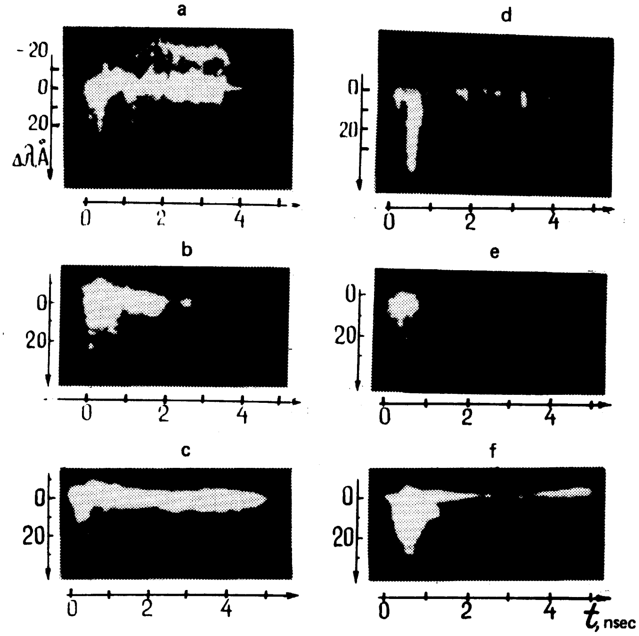

FIG. 6. Time-resolved spectrograms of scattered radiation at the fundamental frequency ω_0 (a, b, c) and at the second harmonic $2\omega_0$ (d, e) for three angles of incidence: a) backscattering; b), d) normal to the target; c), e) specular reflection. Angle of incidence of the target 22.5°.

differences between the spectra although the intensity of the second harmonic in the p-polarization case increased considerably in the specular direction.

V. DISCUSSION OF RESULTS

The main results of our investigation can be summarized as follows.

1. At the beginning of a laser pulse a considerable broadening of the spectrum in the red direction was observed for a period of 1–3 nsec both at the fundamental frequency and at the second harmonic.[1)] This broadening was observed for all the angles of incidence and for all the angles of observation (measurements of the scattering spectrum of the radiation at the frequency $2\omega_0$ were reported earlier[9] and it was found that in the range $q > 10^{14}$ W/cm^2 the broadening up to 25 Å in the red direction was observed at the beginning of a pulse). The degree of broadening at the fundamental frequency reached 70 Å for normal incidence. A distinct fine structure with $\Delta\lambda \sim 1-3$ Å was observed in the spectrum.

2. The blue component was observed only in the backscattered radiation for all the angles of incidence and its intensity increased during a pulse.

3. In the normal incidence case the red part of the spectrum of the backscattered radiation was largely depolarized, whereas the blue part had the polarization of the incident radiation.

4. In the case of oblique incidence there was a relatively narrow line at the unshifted frequency in the specular reflection direction. Measurements carried out using a higher spectral resolution revealed motion of a critical-density layer in the plasma.[9]

5. The intensity of the scattered radiation exhibited oscillations at both ω_0 and $2\omega_0$ frequencies.[6]

The results obtained can be explained by the three main processes occurring in a laser plasma: reflection from a plasma of critical density, reemission of Langmuir waves from a region of critical density, and stimulated Brillouin scattering.

1. Oblique incidence of laser radiation on a target makes it possible to identify, in the specular direction, the reflection from a region of critical density. The spectrum obtained along this direction is characterized by a relatively small width (up to 5 Å), it is unshifted in frequency, and its form does not vary greatly with the incident power density q (Fig. 6c).

2. Reemission of Langmuir waves (l) involves their decay and coalescence ($l \pm s \to t'$) with acoustic waves (s), as described in Refs. 11 and 12. Since Langmuir waves create also radiation at the frequency of the second harmonic because of the processes $l + l' \to t'$ and $l + t \to t'$, the reemission spectrum should be observed simultaneously with the $2\omega_0$ spectrum. Our experiments indicate that the red wing appears in the ω_0 and $2\omega_0$ spectra simultaneously at the beginning of a laser pulse. We can therefore conclude that the frequency ω_0 in this part of the spectrum appears because of reemission of Langmuir waves. The appearance of Langmuir waves because of parameteric instabilities is indicated by the fairly strong isotropy of the reemitted light and by the threshold nature of the process.

Broadening of the spectrum in the course of reemission is[11,12]

$$\Delta\lambda_n = 1.2\cdot 10^{-2}\lambda_0\left[\frac{z/A}{1+0.13\ln(T_e^{1/2}\lambda_0/z)}\right]^{1/2}\cdot 4^{1-n}, \quad (1)$$

where n is the harmonic number and $\lambda_0 = 1.06\ \mu$. For our parameters, we obtain from Eq. (1) $\Delta\lambda_1 \approx 90$ Å and $\Delta\lambda_2 \approx 22$ Å, in satisfactory agreement with the observed values.

Since the red wing in the spectrum is observed at various angles for the normal and oblique incidence, we may conclude that the distribution of Langmuir waves between various directions is fairly isotropic. This is indicated also by the observed depolarization in the red part of the spectrum of the backscattered radiation.

The fine structure in the spectrum of the red wing is possibly a consequence of the transient nature of the Langmuir turbulence. This is supported also by oscillations of the intensity of the scattered radiation.[2)] These oscillations can be explained by deformation of the density profile of the corona near the critical concentration. Even small changes in the density gradient can alter significantly the instability thresholds and this is manifested in the scattering spectra.

The disappearance of the red wing in the scattering spectrum indicates a change in the conditions for the development of the Langmuir turbulence. An increase in the plasma flow velocity may give rise to self-limitation of the field in the vicinity of the critical density region.[6,13] Ponderomotive forces may establish a density profile with a steeper fall in the vicinity of the critical point and this should increase the parametric instability threshold.

3. In the stimulated Brillouin scattering the frequencies of the scattered waves differ from ω_0 by an amount equal to the frequency of the acoustic waves generated in the plasma. In an expanding inhomogeneous laser plasma the frequencies of the acoustic waves are different in different parts of the corona and this results in broadening of the spectrum of the scattered waves.[16] In particular, if the expansion is of the steady-state type, the backscattered light wavelengths λ' differ from the wavelength of the incident light λ_0 by the amount

$$\delta\lambda = \lambda' - \lambda_0 = \frac{4\pi s}{\omega_0}(1-M)[1-(n/n_c)]^{1/2}, \quad (2)$$

where $M = u/s$ is the Mach number, u is the plasma flow velocity along the laser beam axis, $s = 3.11 \times 10^7 (T_e z/A)^{1/2}$ (cm/sec) is the velocity of sound, and z/A is the effective ratio of the charge and atomic numbers for the target material. It follows from Eq. (2) that the red part of the spectrum originates from the part of the corona with the subsonic flow velocity ($M < 1$), whereas the blue part of the spectrum originates from the region with supersonic flow ($M > 1$).

In our experiments the stimulated Brillouin scattering may be responsible for the radiation characterized by a small frequency shift in the red direction and for the blue part of the spectrum. The delay in the appearance of the blue part of the spectrum (Fig. 4a) can be explained by the fact that the plasma expansion velocity increases during a laser pulse. Consequently, beginning from a certain moment in time the scattering is concentrated in the region of supersonic flow ($M > 1$). If the blue edge $\delta\lambda_b$ of the spectrum is formed in the rarefield part of the corona where $(n/n_c) < 1$, we can use Eq. (5) to find readily the March number $M = 1 - \delta\lambda_b c/2\lambda_0 s$. In the case of our polyethylene targets ($z/A \sim 1/2$, $T_e \sim 1$ keV, $\delta\lambda_b = 25$ Å), we have $M \approx 3$.

An increase in the observation angle reduces the influence of the plasma motion on the shift $\delta\lambda$ and the stimulated Brillouin scattering spectrum shifts toward the red wavelengths (relative to the backscattered radiation). This is confirmed qualitatively by the spectrum observed at the angle of 22° (Fig. 4c).

The polarization of the radiation scattered by the stimulated Brillouin effect is mainly the same as the polarization of the incident light. This conclusion is confirmed by the results of our determination of the polarization of the blue part of the spectrum (Fig. 5b).

VI. CONCLUSIONS

Our investigation of the scattered radiation near the frequencies ω_0 and $2\omega_0$ has clearly revealed three main mechanisms governing the scattering and the fundamental frequency: 1) classical reflection from a plasma of critical density; 2) absorption and reemission of Langmuir waves; 3) stimulated Brillouin scattering.

The proposed interpretation of the results allows us to draw certain conclusions on the dynamics of a plasma corona when the power density of the incident radiation is $q > 10^{14}$ W/cm^2. During the initial period (1–2 nsec) the scale of the inhomogeneity in a critical-density region is fairly large and the plasma flow velocity is relatively low ($u < s$). The corona changes with time, the plasma flow velocity increases to $M > 3$, the concentration becomes $n \sim (0.3-0.1)n_c$, and the inhomogeneity scale probably decreases in the critical density region.

In the work of Yamanaka *et al.*[2] the experimental conditions were similar to ours and the broadening of the scattering spectrum near ω_0 was attributed to phase self-modulation of laser radiation in a plasma. However, estimates obtained in Refs. 2 and 17 indicate that the observed spectral broadening ($\Delta\lambda \sim 10$ Å) can be explained only if one assume the existence of a very extended plateau ($L \sim 100\ \mu$) near n_c or a considerable increase in the power density of the laser radiation in the critical density region. This requires experimental verification.

[1)]A wide pedestal in the scattering spectrum at a frequency $2\omega_0$ was first observed without time resolution in Ref. 10.

[2)]Time oscillations of the scattered radiation were observed without spectral resolution in Refs. 14, 15, and 18.

[1]B. H. Ripin, J. M. McMahon, E. A. McLean, W. M. Manheimer, and J. A. Stamper, Phys. Rev. Lett. 33, 634 (1974).

[2]C. Yamanaka, T. Yamanaka, J. Mizui, and N. Yamaguchi, Phys. Rev. A 11, 2138 (1975);

[3]V. Yu. Bychenkov, Yu. A. Zakhorenkov, O. N. Krokhin, A. A. Rupasov, V. P. Silin, G. V. Sklizkov, A. N. Starodub, V. T. Tikhonchuk, and A. S. Shikanov, Pis'ma Zh. Eksp. Teor. Fiz. 26, 500 (1977) [JETP Lett. 26, 364 (1977)].

[4]V. V. Aleksandrov, M. V. Brenner, V. D. Vikharev, V. P. Zotov, N. G. Koval'skiĭ, M. I. Pergament, and V. N. Yufa, Preprint No. IAÉ-2852, Kurchatov Institute of Atomic Energy, Moscow, 1977.

[5]L. M. Gorbunov, Yu. S. Kas'yanov, V. V. Korobkin, A. N. Polyanichev, and A. P. Shevel'ko, Pis'ma Zh. Eksp. Teor. Fiz. 27, 242 (1978) [JETP Lett. 27, 226 (1978)].

[6]N. E. Andreev, V. L. Artsimovich, Yu. S. Kas'yanov, V. V. Korobkin, V. P. Silin, and G. L. Stenchikov, Pis'ma Zh. Eksp. Teor. Fiz. 31, 639 (1980) [JETP Lett. 31, 603 (1980)].

[7]A. L. Egorov, V. V. Korobkin, and R. V. Serov, Kvantovaya Elektron. (Moscow) 2, 513 (1975) [Sov. J. Quantum Electron. 5, 291 (1975)].

[8]B. H. Ripin, J. A. Stamper, E. A. McLean, and F. C. Young, NRL Report No. 7838, 1974.

[9]L. M. Gorbunov, Yu. S. Kas'yanov, V. V. Korobkin, A. N. Polyanichev, and A. P. Shevel'ko, Preprint No. 126, Lebedev Physics Institute, Academy of Sciences of the USSR, Moscow, 1979.

[10]M. Decroisette, B. Meyer, and Y. Vitel, Phys. Lett. A 45, 443 (1973).

[11]L. V. Krupnova, V. P. Silin, and V. T. Tikhonchuk, Fiz. Plazmy 5, 426 (1979) [Sov. J. Plasma Phys. 5, 242 (1979)].

[12]V. Yu. Bychenkov, A. N. Erokhin, and V. P. Silin, Kvantovaya Elektron. (Moscow) 6, 2199 (1979) [Sov. J. Quantum Electron. 9, 1287 (1979)].

[13]N. E. Andreev, V. P. Silin, and G. L. Stenchikov, Zh. Eksp. Teor. Fiz. 78, 1396 (1980) [Sov. Phys. JETP 51, 703 (1980)].

[14]N. G. Basov, O. N. Krokhin, V. V. Pustovalov, A. A. Rupasov, V. P. Silin, G. V. Sklizkov, V. T. Tikhonchuk, and A. S. Shikanov, Zh. Eksp. Teor. Fiz. 67, 118 (1974) [Sov. Phys. JETP 40, 61 (1975)].

[15]Yu. S. Kas'yanov, V. V. Korobkin, P. P. Pashinin, A. M. Prokhorov, V. K. Chevokin, and M. Ya. Shchelev, Pis'ma Zh. Eksp. Teor. Fiz. 20, 719 (1974) [JETP Lett. 20, 333 (1974)].

[16]L. M. Gorbunov and A. N. Polyanichev, Fiz. Plazmy 5, 566 (1979) [Sov. J. Plasma Phys. 5, 316 (1979)].

[17]J. Mizui, H. B. Kang, N. Yamaguchi, T. Sasaki, K. Yoshida, T. Yamanaka, and C. Yamanaka, J. Phys. Soc. Jpn. 41, 1334 (1976).

[18]T. P. Donaldson, M. Hubbard, and I. J. Spalding, Phys. Rev. Lett. 37, 1348 (1976).

Translated by A. Tybulewicz